

# AB INITIO CORE-LEVEL SHIFTS IN METALLIC ALLOYS

Vincenzo Fiorentini,<sup>1</sup> Michael Methfessel,<sup>2</sup> and Sabrina Oppo<sup>1</sup>

(1) *INFM – Dipartimento di Scienze Fisiche, Università di Cagliari, Italy*

(2) *Institut für Halbleiterphysik, P.O. Box 409, D-15204 Frankfurt/Oder, Germany*

## ABSTRACT

Core-level shifts and core-hole screening effects in alloy formation are studied *ab initio* by constrained-density-functional total-energy calculations. For our case study, the ordered inter-metallic alloy MgAu, final-state effects are essential to account for the experimental Mg 1s shift, while they are negligible for Au 4f. We explain the differences in the screening by analyzing the calculated charge density response to the core hole perturbation.

## INTRODUCTION: AB-INITIO CALCULATIONS OF CORE-LEVEL SHIFTS

Core levels are in a way the fingerprints of atoms. Since core levels are affected by the environment surrounding the atom, the observation of their relative position, *i.e.* of core-level *shifts* [1], allows to analyze the charge transfer and structural changes undergone by the atoms when a crystal is formed [2], when an atom is at the surface [3] rather than in the bulk of a solid, or when an alloy is formed out of two elemental solids [4, 5].

In the case of alloy formation (the subject of this paper), a major objective has been to determine the charge transfer between the constituents. Clearly, charge moving from one atom to another causes potential shifts at the atomic sites, which modify the core level binding energies. However, the relation between these shifts and some measure of the charge transfer is not unambiguous. In the simplest form of the “potential model”, the change in the average potential felt by a core electron in a binary compound with a valence charge transfer  $\Delta q$  is taken as

$$\Delta V = \Delta q (k - M) \quad (1)$$

where  $k$  and  $M$  describe the intra- and inter-atom responses, respectively [5]. Thus,  $k$  is similar to a Hubbard  $U$  parameter and  $M$  is a Madelung contribution. These parameters can be estimated from other known quantities, but this involves guesswork and is made difficult by the cancellation between  $k$  and  $M$ . More importantly, the potential model of Eq. (1) is only valid for the “initial state” picture, *i.e.* to describe the positions of the core levels in the alloy and the pure metal *before* a core electron is removed. To compare to the measured binding energies, a final-state screening contribution must be taken into account. This can be included in the formalism only by adding yet another parameter to the model.

It seems thus desirable to make a detailed analysis of a typical system using a method which can quantify the various contributions unambiguously. In the present work, we use *ab-initio* density-functional total-energy calculations to study the MgAu alloy, for which accurate core level shifts have been measured. By studying an effectively isolated excited atom, the screening of the core hole by the valence electrons is described correctly. The core-level shift is cleanly separated into initial-state and final-state relaxation contributions, which can then be checked against the appropriate models. In addition, direct inspection of densities of states (DOS), on-site charges, and screening charge distributions gives an understanding of the effects of alloying, and the different screening responses to a core hole.

Ultimately, we find that the final-state contribution is very important, as it changes both the sign and the magnitude of the core-level shift on the Mg atom. The screening of the Mg

1s core hole is substantially less effective in the alloy than in the pure Mg metal. In turn, the change in screening can be attributed to the reduced Mg valence charge in the alloy. This secondary consequence of the Mg-to-Au charge transfer is at least as important as the direct effect on the initial-state core levels. The initial-state core-level shifts turn out to be compatible with a simple rigid-band model.

*Calculation of core-level shifts* – In the measurement of core-level binding energies, an electron is emitted from the core state into the vacuum. In a metal, another electron moves in to screen the positive charge of the core hole. The reservoir providing the screening electron is that of the valence electrons of the surrounding infinite crystal. Effectively then, the core electron has been lifted to the Fermi level  $E_F$ . Therefore the initial-state estimate of the core binding energy is the position of the core eigenvalue relative to  $E_F$  (not relative to the vacuum potential). The energy relevant to spectroscopic observation (the measured binding energy of the core state including final-state [6] screening effects) can be expressed as the difference in total energy before and after emission of the core electron. The electronic system is neutral and in equilibrium subject to each prescribed core occupation, with the screening electron added to the valence band in the case of a core hole.

The *ab initio* theoretical analysis of the final-state core binding energies is difficult: the presence of a core hole breaks the translational symmetry of the lattice, requiring the use of appropriate supercells where the core hole is decoupled from its periodic images, or of equivalent treatments. Also, it is imperative to allow for self-consistency of the charge rearrangement around the core hole. The alloy core-level shift, including final-state relaxation effects, is calculated as

$$\Delta = [E_{\text{TOT}}^{\text{alloy}}(q = 1) - E_{\text{TOT}}^{\text{alloy}}(q = 0)] - [E_{\text{TOT}}^{\text{const}}(q = 1) - E_{\text{TOT}}^{\text{const}}(q = 0)], \quad (2)$$

where the total energies of supercells of the alloy and the pure constituent elements are evaluated for one electron and no electron ( $q = 1$  and  $q = 0$ , respectively) promoted out of the relevant core level to the valence band. For an accurate DFT calculation, the resulting shift should be close to the experimental value. The initial-state estimate is obtained by comparing the core eigenvalues relative to  $E_F$  for the two systems. The difference of the full and initial-state results is, by definition, the final-state screening contribution. In this context, it is advantageous to use an all-electron method, which gives direct information on core electron levels. Note that surface properties (specifically, the work function) do not enter either description. This must be the case for an acceptable model: *the exact core binding energy, expressed as the difference of two total energies, is a bulk property.*

Our self-consistent electronic-structure and total-energy calculations were done with the all-electron full-potential LMTO method [7], within the local approximation (LDA) to density-functional theory (DFT) [8]. Minimization of the energy under a constrained core occupation is rigorously justified [9] in the DFT framework: a self-consistent calculation under the chosen constraint provides a variational total energy in the parameter subspace identified by the constraint, and the rigorous definition of core level shifts as differences of total energies can be applied. To calculate the final-state core-level shifts, we perform total-energy calculations at various occupations of the relevant core state in appropriate supercells (see below).

*Connection between initial-state and exact core-level shifts* – Within DFT, one can adopt an approach similar to Slater’s transition-state concept [10], which adds to our understanding of final-state effects. This is based on Janak’s formula [11], which for the present purposes

can be restated as

$$\frac{\partial E_T}{\partial q} = E_F - E_c(q) \equiv \epsilon_c(q), \quad (3)$$

where  $E_F$  is the Fermi energy,  $E_c$  is the core-level eigenvalue, and  $q$  is the promoted charge. If we assume that the core level energy varies linearly with the occupation of the level (a good approximation), the total-energy difference of Eq.2 can be expressed via trapezoidal-rule integration of Eq.3 between zero and unit promoted charge, as

$$\begin{aligned} \Delta &\approx \frac{1}{2} \left\{ [\epsilon_c^{\text{alloy}}(1) + \epsilon_c^{\text{alloy}}(0)] - [\epsilon_c^{\text{const}}(1) + \epsilon_c^{\text{const}}(0)] \right\} \\ &\approx \Delta_I + \frac{1}{2} \left\{ [\epsilon_c^{\text{alloy}}(1) - \epsilon_c^{\text{alloy}}(0)] - [\epsilon_c^{\text{const}}(1) - \epsilon_c^{\text{const}}(0)] \right\} \end{aligned} \quad (4)$$

where the second line rephrases the alloy core-level shift as a correction to the initial-state estimate  $\Delta_I = \epsilon_c^{\text{alloy}}(0) - \epsilon_c^{\text{const}}(0)$ . This identifies the correction due to final-state screening effects as the difference of core eigenvalue *drop* upon depopulation of the level in the two environments. The above description helps to make contact to differences in the screening response of the two environments in question. In general terms, the eigenvalue of the depopulated core state drops by a larger amount when the valence electrons screen the core hole less efficiently.

Formally, the occupation of a state can be varied continuously in DFT, which allows self-consistent calculations at arbitrary occupation. Therewith one can verify that the total energy derivative (Eq.3) is very nearly linear in the occupation number of the state. The second derivative of the total energy vs. promoted charge is positive, which of course indicates that at non-zero promoted charge the system is unstable towards reoccupation of the state [12]. This, however, does not affect the variational character of the total energy under each occupation constraint [9].

## A CASE STUDY: MgAu

We applied the technique outlined above to the core shifts of the Mg 1s and Au 4f levels upon formation of the binary, CsCl-structure MgAu alloy (assumed to be ordered) out of bulk Au and Mg. Accurate experimental data [4, 5] exist for the core level shifts upon formation of this alloy. The calculated structural parameters for MgAu, Au and Mg are given in Table I. The results for these bulk systems are of standard DFT-LDA quality. For Mg, the fcc structure was adopted.

	$a_0$ (bohr)	$B_0$ (Mbar)	$E_{\text{coh}}$ (eV/atom)
MgAu th.	6.09	1.05	3.70
MgAu exp.	6.15	—	—
Au th.	7.68	1.85	4.33
Au exp.	7.70	1.73	3.81
Mg th.	8.38	0.40	1.69
Mg exp.	8.46	—	—

Table I: Structural properties of MgAu (CsCl structure), Au (fcc) and Mg (fcc). Cohesive energy do not include spin-polarization. The Mg experimental lattice constant corresponds to the experimental volume per atom in the hcp structure.

To study the core-hole-excited solids, we used 16-atom supercells for both CsCl-structure MgAu, and fcc Mg and Au. The distance of the core hole from its periodic images exceeds

12 bohr in all cases, and tests show that our values for the core level shifts are converged with respect to cell dimension. The localization of the calculated density response provides an *a posteriori* justification for the supercell approach. The Brillouin-zone integration was done using more than 50 irreducible special points. Muffin-tin radii for Mg (Au) are 2.94 (2.60) bohr in the pure metal and 2.50 (2.70) in the compound at the experimental lattice constants, and are scaled with the lattice constant. All the calculations are scalar-relativistic.

As already mentioned, the core eigenvalues extracted from bulk calculations provide the initial-state estimate of the core shifts (see text after Eq. 4). An electron is then removed from each core state of interest in each of the bulk supercells, and the full “final-state” core level shifts are obtained as total energy differences. Using fractional occupation, we verified the linear behaviour of  $\epsilon_c$ , and the validity of the Slater transition state rule.

The results of the calculations in the different approximations are summarized in Table II, and compared with the experimental values of Ref. [5]. The full results are in very good agreement with experiment for both cases. The initial-state estimate is accurate for the Au 4*f* shift, but it is incorrect in sign and magnitude for Mg 1*s*. The screening contributions to the shifts are thus completely different in the two cases: negligible for Au, very substantial for Mg. This is a valuable piece of information provided by the *ab initio* calculation. While

shift	exp	full	initial	screening
Au 4 <i>f</i>	0.74	0.73	0.74	0.01
Mg 1 <i>s</i>	0.34	0.25	−0.44	0.69

Table II: Mg 1*s* and Au 4*f* core-level shifts in MgAu with respect to Au and Mg bulk. All values are in eV. Column “full” is the full calculation, column “initial” is the initial-state shift (difference of core eigenvalues at zero promoted charge), column “screening” is the difference of the previous two, and is the contribution due to screening effects. Experimental data from Ref.[5].

appropriate for Au, the initial-state approximation gives a qualitatively incorrect picture of the Mg 1*s* shift. This is due to the differences in the screening response at the Mg site in the alloy as compared to the elemental bulk. The positive shift (obtained from both full final-state calculation and experiment) means that the core eigenvalue drops more strongly when depopulated in the alloy than in elemental Mg. So the screening response to the core-hole perturbation at the Mg site is less effective in the alloy than in Mg bulk: clearly, this could not be inferred from an initial-state or model estimate. Note that even the

case	exp	calc
Au 4 <i>f</i> in Au bulk	85.88	85.78
Au 4 <i>f</i> in MgAu	86.62	86.51
Mg 1 <i>s</i> in Mg bulk	1303.20	1306.78
Mg 1 <i>s</i> in MgAu	1303.54	1307.03

Table III: Calculated vs. measured core-level binding energies, in eV, referred to the Fermi level. Experiment: Ref.[5]

*absolute* core binding energies (referred to  $E_F$ , and obtained as total-energy differences) are in remarkable agreement with experiment. Errors are well below 1%, as can be seen in Table III. This may be not too surprising, since the core levels are obtained as differences of two exact (within DFT-LDA) total energies.

Also, we mention that the solid with a core hole is the initial-state configuration for the primary-hole recombination with ensuing emission of the Auger electron [13]. The initial-

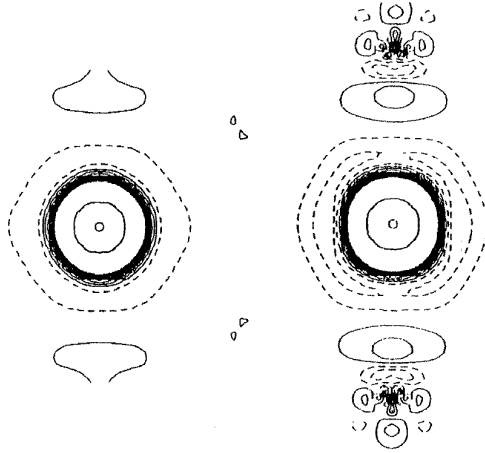


Figure 1: Screening charge density for a  $4f$  core hole at the Au site in MgAu (left) and in Au bulk (right). All pictures drawn on the same scale. Solid (dashed) line: positive (negative) values.

state estimate of the Mg→MgAu shift of the  $KLL$  Auger transition extracted from our calculated eigenvalues in the core-hole-excited solid is 1.3 eV, which compares reasonably with the experimental value of 1.0 eV [5]. (Of course, this agreement may result from the cancellation of multiple-core-hole [1, 13] relaxations.)

*Initial-state shifts* – Initial-state-based models, used to infer charge transfer from core-level shifts, rely implicitly on a rigid-band picture: a shift of the DOS of the constituents is related to charge transfer from one species to another. Assuming that core levels move rigidly along with the valence DOS, an estimate of the charge transfer from species 2 to 1 is

$$\Delta q^{(1)} \equiv D_F^{(1)} \Delta \epsilon_c^{(1)} = D_F^{(2)} \Delta \epsilon_c^{(2)} \equiv -\Delta q^{(2)}$$

where  $D_F$  is the DOS at the Fermi level, and  $\Delta \epsilon_c$  is the core level shift. The core shift measures, via the Fermi-level DOS, the amount of depletion or filling of the valence DOS, *i.e.* the charge transfer. Our initial-state results agree with this simple picture. Using calculated initial-state shifts and Fermi-level DOS, we get opposite sign and about equal moduli of the  $\Delta q$ 's:  $-0.195$  electrons for Mg, and  $0.199$  for Au, which are reasonable estimates of the charge transfer. Of course, this picture is insufficient to account for the full results, which contain a large screening contribution.

*Final-state screening contribution* – To understand the environment dependence of the screening, we examine differences of total charge densities of the perturbed and the unperturbed supercells of the three materials around an excited Mg or Au atoms: these differences are the response or screening density. The response density of Au bulk to the Au  $4f$  core excitation is very localized, and due mostly to the transition-metal-like screening of the  $5d$  electrons (right panel in Fig. 1). The Au  $d$ -shell contains 10 electrons both before and after the core hole is created. Our picture for the Au screening is that the  $d$  shell moves closer to the nucleus, leaving behind a charge-depleted ring; the screening electron from valence  $sp$  states fills up this ring. In the MgAu alloy, the screening is almost identical to that in Au bulk, very short-ranged and dominated by the  $d$  shell (left panel of Fig. 1); accordingly, the core shift has practically no screening-related contribution, and the initial-state estimate is accurate. This is in full agreement with both calculation and experiment.

As was to be expected, in bulk Mg the response density to a Mg  $1s$  hole is a roughly spherical screening lump of  $sp$  nature (Fig. 2, right panel); its extension is normal on

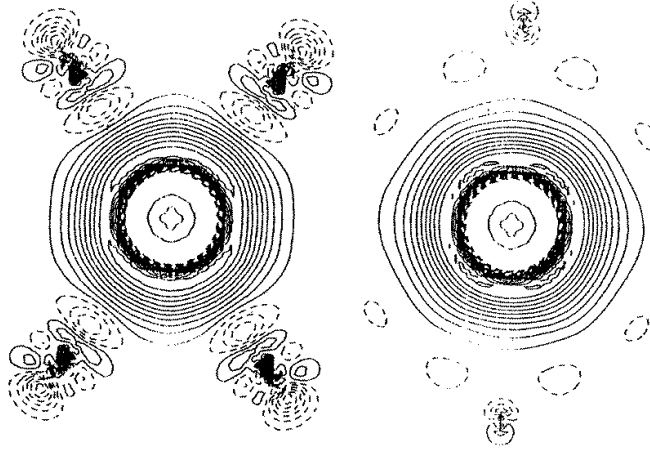


Figure 2: Screening density for a 1s hole at the Mg site in MgAu (left) and in Mg bulk (right).

the scale of the Mg-Mg interatomic distance in the bulk, but appreciably larger than that of the response density around Au in its own bulk. Since the interatomic distances are  $d_{\text{Au-Au}} = 5.43$  bohr in Au,  $d_{\text{Mg-Mg}} = 5.92$  bohr in Mg, and  $d_{\text{Au-Mg}} = 5.27$  bohr in MgAu, we expect sensitivity of the spatially-extended screening response of Mg to the surrounding environment in MgAu. Indeed this is the case, as seen in Fig.2. Now, there are two basically different ways of interpreting the final-state effects for Mg. **First:** alloying changes the properties of the unexcited Mg atom (essentially, by charge transfer); only this modified screening ability of the Mg atom matters. For Mg, there is less screening charge spread out over the atomic volume than in the bulk constituent, which reduces the screening efficiency. The site-projected density of states at the Fermi level has also decreased (by a factor of 2), and this again reduces the available “mobile” charge. **Second:** concurrently to the first mechanism, the Mg screening charge extends far enough as to be sensitive to the its neighborhood. Charge is subtracted by the neighbors to the screening lump, making the response less efficient.

The second explanation is tempting in view of the screening response shape in Fig.2 (left). While in Mg bulk (right panel) only Mg atoms relatively far from the excitation site are present, in MgAu eight polarizable Au neighbors surround the excited Mg site at an appreciably ( $\sim 10\%$ ) shorter distance. Contour counting in Fig.2 already suggests that the screening charge at the core-hole is partially depleted. This also results from the integrated screening charges  $Q_{\text{scr}}$  within spheres surrounding the core-hole site. Assuming sphere radii of 2.48 bohr for Au and 2.68 a.u for Mg, one gets  $Q_{\text{scr}} = 0.840$  and 0.680 electrons for Mg in Mg bulk and MgAu, respectively. The depletion in the alloy results in a large positive contribution to the shift, as calculated and observed. For Au,  $Q_{\text{scr}} = 0.845$  and 0.821 electrons in Au bulk and MgAu respectively. (Of course, integrated charges within spheres are to some extent arbitrary, and should only be taken as qualitative indicators.)

On the other hand, while the density response is undoubtedly modified by the neighbors, most of the difference in screening response comes from within the Mg atom. Most of the spherically-averaged Mg-to-MgAu difference of screening potential around the Mg site (whose integral gives the value of the potential shift at the nucleus) is bounded within half interatomic distance, although it remains non zero outside as well. We suggest that it is a combination of the two mechanisms just outlined that causes the screening deterioration at the Mg site in MgAu, the bulk of it being due to pure charge transfer, with comparatively

minor effects caused by shape and extension of the screening response density.

*Antiscreening around Mg in MgAu* – While possibly not central to the understanding of the screening contribution to the Mg 1s shift, the “antiscreening” feature on Au neighbors visible in the Mg 1s density response in Fig. 2, right panel, is quite interesting. We suggest that it may be interpreted as follows. The Friedel oscillation wavelength for an electron gas having the average density of Mg ( $\bar{\rho} = 0.024 \text{ bohr}^{-3}$ ), is  $\lambda = 3.7 \text{ bohr}$ , while it is  $\lambda = 2.2 \text{ bohr}$  at the higher density of Au ( $\bar{\rho} = 0.098 \text{ bohr}^{-3}$ ). We may then roughly picture the response charge around Mg as a blob of Mg-density (low) electron gas surrounded at close distance by blobs of Au-density (high) electron gas. The screening wavelength around Mg gets shorter (more akin to a high-density gas), approaching the efficiently-screening Au sites: we name this a variable-wavelength Friedel oscillation of the core-hole screening density.

## SUMMARY

Results of realistic, fully *ab initio* density-functional theory calculations of core level shifts have been presented for the Mg 1s and Au 4f bulk-to-alloy shifts upon formation of the MgAu intermetallic alloy. A large screening contribution was found for the Mg 1s shift, whereas the same contribution is negligible for Au 4f. We observed unusual features in the screening around an excited Mg atom in MgAu, and suggested a physical picture in terms of variable-wavelength Friedel oscillation around the Mg core hole, caused by the neighboring Au atom in the alloy.

The *ab initio* treatment provides useful information about alloy core-level shifts, which could not be obtained from experiment or models: calculated core-level shift accurately reproduce experiment; theory can quantify initial-state and screening contributions separately; initial-state shifts are found to be compatible with a rigid-band model; screening densities at excited Au and Mg atoms enable to understand final-state contributions; charge transfer is the central control parameter for the shifts.

## REFERENCES

- [1] W. F. Egelhoff, Surf. Sci. Rep. **6**, 253 (1987).
- [2] A. R. Williams and N. D. Lang, Phys. Rev. Lett. **40**, 954 (1978).
- [3] B. Johansson and A. Rosengren, Phys. Rev. B **21**, 4427 (1980); A. Rosengren and B. Johansson, *ibid.* **22**, 3706 (1980). M. Methfessel, D. Hennig, and M. Scheffler, Surf. Sci. **287/288**, 785 (1993); M. Alden, H. L. Skriver, and B. Johansson, Phys. Rev. Lett. **71**, 2449 (1993).
- [4] G. K. Wertheim *et al.*, Phys. Rev. B **20**, 860 (1979).
- [5] T. D. Thomas and P. Weightman, Phys. Rev. B **33**, 5406 (1986).
- [6] G. D. Mahan, *Many-particle physics* (Plenum, New York 199).
- [7] M. Methfessel, Phys. Rev. B **38**, 1537 (1988); M. Methfessel, C. O. Rodriguez, and O. K. Andersen, *ibid.* **40**, 2009 (1989); O. K. Andersen, O. Jepsen, and D. Glötzl, in *Highlights of Condensed Matter Theory*, F. Bassani, F. Fumi, and M. P. Tosi eds., (North-Holland 1985).
- [8] O. Gunnarsson and R. O. Jones, Rev. Mod. Phys. **61**, 689 (1989). We use the LDA exchange-correlation functional by D. M. Ceperley and B. J. Alder, Phys. Rev. Lett. **45**, 566 (1980), as parametrized by S. H. Vosko, L. Wilk, and M. Nusair, Can. J. Phys. **58**, 1200 (1980).
- [9] P. H. Dederichs, S. Blügel, R. Zeller, and H. Akai, Phys. Rev. Lett. **53**, 2512 (1984); O. Gunnarsson and B. I. Lundqvist, Phys. Rev. B **13**, 4274 (1976).
- [10] J. C. Slater, *Quantum theory of molecules and solids-IV* (McGraw-Hill, New York 1974).
- [11] J. Janak, Phys. Rev. B **18**, 7165 (1978).
- [12] See O. A. Pankratov and P. P. Povarov, Phys. Lett. A **134**, 339 (1989).
- [13] P. Weightman, Rep. Prog. Phys. **45**, 753 (1982).